Molecular Dynamics Simulations of Reactions of Hyperthermal Fluorine Atoms with Fluorosilyl Adsorbates on the Si{100}-(2 × 1) Surface

Alema Galijatovic, Adam Darcy, Ben Acree, George Fullbright, Rupert McCormac, Bryan Green, and Kristin D. Krantzman*

Department of Chemistry, College of Charleston, Charleston, South Carolina 29424

Tracy A. Schoolcraft

Department of Chemistry, Shippensburg University, Shippensburg, Pennsylvania 17257

Received: January 2, 1996; In Final Form: March 21, 1996[⊗]

Molecular dynamics simulations of the reactions between gaseous fluorine atoms and $(SiF_x)_n$ adsorbates on the Si{100}-(2 × 1) surface are performed using the SW potential with the WWC reparameterization. The objective of the simulations is to determine how the chemical composition and energy distribution of the etched gas-phase products depend on the identity of the reacting adsorbate. Reactions of normal incident fluorine atoms with SiF_3, SiF_2-SiF_3, and $SiF_2-SiF_2-SiF_3$ adsorbates are simulated at incident kinetic energies from 3.0 to 9.0 eV. SiF_4 is the major product in nearly all cases. An S_N2-like mechanism is responsible for the formation of SiF_4, Si_2F_6, and Si_3F_8. In addition, at 7.0 and 9.0 eV, the simulations have discovered a previously unknown mechanism for the formation of SiF_4, which involves an insertion between a silicon−silicon bond. The simulations predict that radical species are formed predominantly from fragmentation of the higher mass etched products with only a few being formed directly from the reaction between the incoming fluorine atom and the adsorbate. Comparisons are made to experimental data on silicon−fluorine etching with both thermal and hyperthermal fluorine atoms.

I. Introduction

Fluorine atoms are thought to be the primary reactive agents in silicon etching by fluorine plasmas, a process important in the fabrication of microelectronic devices. Consequently, much experimental and theoretical work has focused on elucidating the mechanisms for reactions between fluorine and a silicon surface.[1] A better understanding of the surface reactions responsible for silicon−fluorine etching can be applied to improving methods for the production of microelectronic devices. Recent experiments show that spontaneous silicon−fluorine etching occurs at room temperature with a small reaction probability estimated to be less than 0.01.[2] SiF_4 is the major product with Si_2F_6 and Si_3F_8 as minor products.[1−4] Small amounts of radicals are also observed. The relative amounts of the gas-phase products depend on both surface conditions and the etching species. A higher proportion of Si_2F_6 and Si_3F_8 are observed with fluorine atoms than with F_2 or XeF_2. Products are formed when an incoming fluorine atom reacts with a fluorosilyl layer and ruptures silicon−silicon bonds. Interestingly, experiments suggest that reactions within the fluorosilyl layer do not make a significant contribution to spontaneous etching at room temperature.[1]

Experiments have determined that the reactive fluorosilyl layer is composed of SiF, SiF_2, and SiF_3 groups.[5,6] Lo *et al.* studied the reaction between XeF_2 and the Si{111}-(7 × 7) surface. They have concentrated on elucidating the mechanisms responsible for the observed etching products by determining the structure of the reaction layer as the reaction proceeds.[7,8] By using SXPS and PSD spectroscopies, they determined that, during steady-state etching, SiF and SiF_2 groups are in the lower portion of the fluorosilyl layer and the SiF_3 groups are in the top portion. This experimental data further supports the hypothesis by Schoolcraft and Garrison that the reactive layer is composed of tower-like adspecies of SiF and SiF_2 groups terminated by SiF_3 groups.[9] SiF_4 is formed when a fluorine atom abstracts a terminating SiF_3 group, Si_2F_6 is formed when a fluorine atom abstracts SiF_2-SiF_3, and Si_3F_8 is formed when a fluorine atom abstracts $SiF_2-SiF_2-SiF_3$.

Experiments with hyperthermal fluorine atoms have recently been performed by Giapis and co-workers, who have studied the reactions between 4.8 and 6.0 eV fluorine atom beams and $(SiF_x)_n$ adsorbates on the silicon surface.[10,11] Their experiments were with a thin fluorosilyl layer that most likely is composed of SiF_3 and SiF_2-SiF_3 groups. SiF_2, SiF_4, and Si_2F_6 were observed as thermal products. The hyperthermal products are thought to be either SiF_3 or vibrationally excited SiF_4 and SiF_2.

Theoretical work has focused on the use of *ab initio* calculations and molecular dynamics simulations to study reactions between silicon and fluorine. A potential energy function with two-body and three-body terms to model silicon−silicon, fluorine−fluorine, and silicon−fluorine interactions has been developed by Stillinger and Weber (SW).[12−15] The three-body terms are necessary to model the tetrahedral bonding of silicon and silicon fluoride species. Schoolcraft and Garrison have used the SW potential energy function to determine the initial sticking probability of F atoms on the clean Si{100}-(2 × 1) surface and got good quantitative agreement with experiment.[16] In a later paper, they simulated the initial stages of etching of the Si{100}-(2 × 1) surface by 3.0 eV normal incident fluorine atoms.[9] Schoolcraft and Garrison observed a reaction layer consisting of tower-like species of SiF, SiF_2, and SiF_3, which was also observed by Feil *et al.* in similar simulations with chlorine.[17] Schoolcraft and Garrison determined that SiF_4 is produced by an S_N2-like mechanism, which is in agreement with the *ab initio* calculations of Garrison and Goddard.[18] Their product distribution, 54% SiF_3, 35% SiF_4,

* Author to whom correspondence should be addressed. E-mail: kdk@theory.cofc.edu.

⊗ Abstract published in *Advance ACS Abstracts,* May 1, 1996.

S0022-3654(96)00058-5 CCC: $12.00

7% SiF_2, and 4% other, did not agree with the experimental distribution. They attributed this primarily to the fact that they did not maintain maximum fluorine coverage during the simulation and also to deficiencies in the potential energy function. Recently, Barone and Graves have used the SW potential to perform molecular dynamics simulations of low-energy argon-ion bombardment of silicon layers while incorporating fluorine atoms into the reactive layer.[19] They were also able to obtain a reactive layer consisting of treelike structures of SiF, SiF_2, and SiF_3 groups. Simulations by both Feil *et al.*[17] and Barone and Graves[19] show that etching with ion bombardment produces pits in the surface which contain buried silicon−halide species.

In order to change the SW potential to better model adsorption reactions on the Si{100}-(2 × 1) surface, Weakliem, Wu, and Carter (WWC) reparameterized the potential for the silicon−fluorine interactions. They compared the SW potential with *ab initio* data for the interaction of a fluorine atom with a cluster to model the reconstructed silicon surface.[20,21] They found the SW potential to be too repulsive for both adsorption of fluorine on the Si{100}-(2 × 1) surface and for lateral interactions between fluorines. In order to correct for this, the WWC potential was fit to 42 *ab initio* points on the energy surface in addition to the experimental gas-phase data.[20,21] With this potential, Carter and co-workers studied the adsorption probability of isothermal fluorine gas atoms, the initial buildup of the fluorosilyl layer,[20,21] and reactions of F_2 molecules with a clean surface.[22,23] In addition, Schoolcraft *et al*. used both the SW potential and the reparameterized potential to perform a study of the reactions of F_2 molecules with a clean surface.[24]

Previous molecular dynamics simulations of silicon−fluorine etching have focused on the formation of the reactive fluorosilyl layer. The molecular dynamics simulations presented in this paper are unique because they focus on the last step of etching: the reaction between gaseous fluorine atoms and reactive $(SiF_x)_n$ adsorbed species to produce gas-phase products. The objective of the simulations is to determine how the chemical composition and energy distribution of the etched gas-phase products depend on the identity of the reacting adsorbate. Molecular dynamics simulations using the WWC reparameterization of the SW potential are run for the following elementary reactions: F(g) + SiF_3(a), F(g) + SiF_2−SiF_3(a) and F(g) + SiF_2−SiF_2−SiF_3-(a). These adsorbates are chosen because they are thought to be the precursors to the observed products. Five hundred trajectories of each reaction are run at four kinetic energies of the incoming fluorine atom brought in at normal incidence with 3.0, 5.0, 7.0, and 9.0 eV. Experimentally, the kinetic energies of fluorine atoms used in silicon etching have been determined to range from thermal, 0.026 eV, to 8.0 eV.[25] The reaction probability at room temperature is very small, which suggests that it is the very high-energy fluorine atoms at the tail of the Boltzmann distribution that are responsible for spontaneous etching. The simulations are run with higher incident kinetic energies in order to selectively sample these higher energy atoms. The reaction cross section, energy distribution, and effective internal energy of each gas-phase product are determined as functions of both the adsorbate type and the incident kinetic energy. In addition, the mechanisms for the formation of the etching products are elucidated. Si_2F_6 is the only product at 3.0 eV. At and above 5.0 eV, it is found that SiF_4 is the major product in nearly all cases. Furthermore, it has been determined that radical species are formed predominantly from fragmentation of etched products with only a few being formed directly from the reaction between the incoming fluorine atom and the adsorbate.

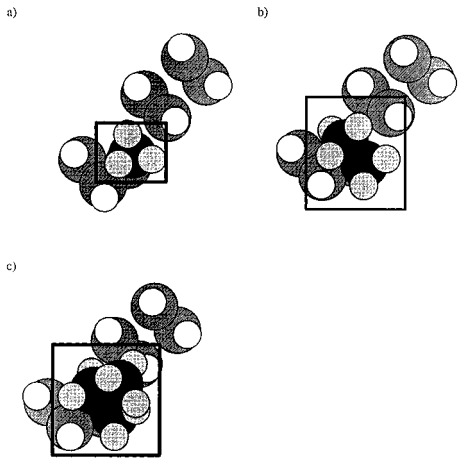

Figure 1. Top view of the adsorbate and surface layer of the microcrystallite. Silicon atoms are the larger diameter spheres, and fluorine atoms are the smaller diameter spheres. The adsorbate is shaded a darker gray. (a) SiF_3 adsorbate; (b) SiF_2−SiF_3 adsorbate; (c) SiF_2−SiF_2−SiF_3 adsorbate.

The organization of the paper is as follows. Section II describes the molecular dynamics simulations, the calculation of the reaction cross section, and the analysis of the products. In section III, the mechanisms for reaction, the reaction cross section, and the energy of the products are presented. In section IV, the meaning and importance of the results are discussed in light of experimental data. Conclusions and a summary of the results of the simulations are in section V.

II. Description of the Calculations

Molecular dynamics are performed in which the reaction between an incoming fluorine atom and the reactive adsorbate is simulated. In order to obtain a statistical distribution, 500 trajectories of each reaction are performed. The details of the simulations are described in section A. The analysis of the simulations is described in section B. Three types of calculations are described: the determination of the trajectory outcome, the calculation of the reaction cross section, and the analysis of the products.

A. Molecular Dynamics Simulation. Molecular dynamics is a method by which the motions of atoms during the course of a chemical reaction may be followed as a function of time. The force on each atom is calculated using a potential energy function, and then the motion is determined by Newton's equations of motion. The main advantages of the method are that it can treat large systems and that it provides a dynamical picture as the chemical reactions occur. The reliability of the simulation is limited primarily by the accuracy of the potential energy function.

The Si{100}-(2 × 1) surface is modeled by a microcrystallite consisting of six layers of silicon atoms with eight atoms per layer that was used by Schoolcraft and Garrison[9] in previous molecular dynamics simulations. The top layer of silicon atoms is reconstructed into dimers, and the dangling bonds of the surface silicon atoms are saturated with fluorine atoms. A surface dimer is replaced with a $(SiF_x)_n$ adsorbate. The structure for each of the adsorbates is determined from previous simulations by Schoolcraft and Garrison of the initial stages of silicon−fluorine etching.[9] Figure 1 shows the surface with the three different adsorbates, SiF_3, SiF_2−SiF_3, and SiF_2−SiF_2−SiF_3.

Initially, the surface is equilibrated at 300 K using an algorithm based on the Generalized Langevin Equation (GLE) to couple the surface to a heat bath that maintains the temperature of the crystal.[26] The bottom layer of atoms is rigid,

and the next four layers of atoms are the stochastic region. Details of the application of this method to the microcrystallite of silicon have been described previously.[9,16] The reaction with the fluorine atom is fast (∼100−200 fs), and therefore, there is not enough time for the energy released by the reaction to dissipate through the crystal before the product desorbs. Consequently, the results of the simulations with and without a heat bath are very similar. Simulations with a larger crystal are performed in order to check that the heat bath is functioning properly. Periodic boundary conditions are applied in the surface plane in order to model an infinite crystal. In order to simulate experiment, both the initial vibrational phase of the crystal and the initial coordinates of the fluorine atom are randomly sampled. Four incident kinetic energies for the fluorine atom, 3.0, 5.0, 7.0, and 9.0 eV, are used in the simulations. The fluorine atoms are brought in at normal incidence with respect to the surface. Five hundred trajectories of each reaction are simulated.

B. Analysis of the Results. *1. Trajectory Outcome*. The three most common outcomes for the interaction of the fluorine atom with the surface are no reaction, adsorption, and etching. At higher kinetic energies, chemically-induced desorption is also observed in which adsorption of the incoming fluorine atom induces desorption of adsorbate atoms from the surface. The trajectory is terminated when one of these four outcomes is determined: no reaction, absorption, etching, or chemically-induced desorption. A fluorine atom is determined to be nonreactive when the potential energy of the atom is zero with respect to the surface and the atom is moving away from the surface. The silicon−fluorine binding energy is 5−7 eV, and therefore, a fluorine atom is determined to be adsorbed when its binding energy is greater than 5 eV and it remains on the surface. When the binding energy of the fluorine atom is greater than 5 eV and its height above the surface is greater than 16 Å, it is determined that the fluorine atom is part of a gas-phase etched product. The etched products are formed in two ways. Most commonly, the incoming fluorine atom reacts directly with the adsorbate to produced an etched product. At higher energies, the incoming fluorine atom occasionally reacts with a mono-fluorinated silicon to form SiF_2.

2. Reaction Cross Section. The reaction probability is determined as the fraction of trajectories that etch. However, the reaction probability cannot be directly compared among different types of adsorbates because each adsorbate has a different surface area. The reaction cross section, in units of square angstroms, is the product of the reaction probability and the surface area available to the incoming fluorine atom. As an example, Figure 2 shows a top view of the SiF_3 adsorbate on the surface. A box is drawn around the area, 14.9 Å^2, that is available to the incoming fluorine atom. Five hundred trajectories are run, and the aiming points of the incoming fluorine atom that produce SiF_4 are plotted. Only 19 of the 500 trajectories etch, and therefore, the reaction cross section is (14.9 Å^2)(19/500) = 0.6 Å^2. The reaction cross section measures the actual area of the adsorbate that is reactive and can be compared among different types of adsorbates. When the aiming points of the fluorine atom are sampled over the entire microcrystallite, very few trajectories result in reaction. By decreasing the sampling area to the area just around the adsorbate, the effective reaction probability is significantly increased so that more products can be examined. The sampling area used with each adsorbate is chosen so that all possible etching trajectories are included. A sampling area of 14.9 Å^2 is used with SiF_3, 39.3 Å^2 is used with SiF_2−SiF_3 and 40.8 Å^2 is used with SiF_2−SiF_2−SiF_3. Boxes to illustrate the sampling areas are shown around each adsorbate in Figure 1.

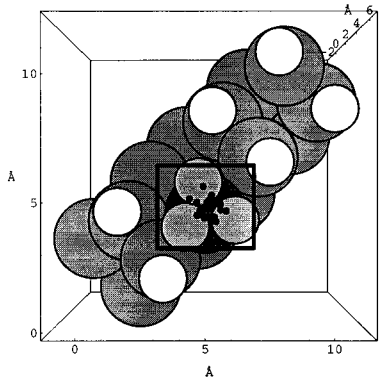

Figure 2. Pictorial representation of the reaction cross section, which is the reactive area of the adsorbate in Å^2. A top view of the SiF_3 adsorbate is shown. A box is drawn around the surface area available to the incoming fluorine atom. The aiming points out of 500 that etch SiF_4 are plotted as black points. The reaction cross section is the product of the fraction of trajectories that etch with the surface area.

3. Analysis of the Products. When a fluorine atom is determined to have etched the surface, the etched product is analyzed by collecting the coordinates of all atoms above the surface. The potential energy of these atoms is calculated and is used to identify the product, and the coordinates of the product are performed as an additional check, in which each coordinate is rendered as a sphere and the product is identified visually.

The analysis of the energy distribution of the product is begun when the molecule has a constant center of mass translational energy which is ∼12 Å above the surface. The average total kinetic energy and average potential energy of the product are determined from time averaging over ∼500 fs. The internal energy of the product is obtained by subtracting the center of mass translational energy from the total kinetic energy of the molecule: $E_{int} = E_{kin} - E_{cm}$. The effective internal energy, E_{eff}, is a measure of the stability of the gas-phase product. It is calculated as $E_{eff} = V(r_{ij}) + ke(r_{ij}) - V_{eq} - E_{diss}$.[27] $V(r_{ij})$ and $ke(r_{ij})$ are the potential energy and kinetic energy of the product relative to the center of mass, V_{eq} is the potential energy of the product in its equilibrium configuration, and E_{diss} is the energy needed to break the weakest bond in the molecule. V_{eq} is determined by slowly reducing the temperature of the molecule to 0 K using an algorithm based on the GLE[26] and then calculating the potential energy with the resulting coordinates. The dissociation energy for a bond is determined as the difference between V_{eq} of the molecule and V_{eq} of the fragments after the bond is broken. Using the SW potential with the WWC parameterization, the silicon−fluorine bond energy of SiF_4 is determined to be 6.4 eV, the silicon−silicon bond energy in Si_2F_6 is 4.4 eV, and the silicon−silicon bond energy is 4.0 eV for Si_3F_8. If E_{eff} is greater than zero, the molecule has enough energy to dissociate and the product will fragment.

4. ΔE for $F(g) + (SiF_x)_n(a) \rightarrow$ Gas-Phase Products. In order to better understand the energetics of these reactions, the WWC reparameterization of the SW potential is used to calculate ΔE for each of the major reactions under study. ΔE is calculated by subtracting V_{eq} of the reacting surface from the sum of V_{eq} of the final surface and V_{eq} of the gas-phase product. In each reaction, one silicon−silicon bond is broken and one silicon−fluorine bond is formed. Gas-phase data predicts an energy difference of approximately −2.0 eV. Table 1 shows ΔE for reactions on the surface. The reactions on the surface are more exothermic than those predicted by gas-phase data.

TABLE 1: ΔE for F(g) + $(SiF_x)_n$(a) → Gas-Phase Products[a]

reaction	ΔE (eV)
$F(g) + SiF_3(a) \rightarrow SiF_4(g)$	−4.6
$F(g) + SiF_2{-}SiF_3(a) \rightarrow SiF_4(g)$	−4.6
$F(g) + SiF_2{-}SiF_3(a) \rightarrow Si_2F_6(g)$	−5.8
$F(g) + SiF_2{-}SiF_2{-}SiF_3(a) \rightarrow SiF_4(g)$	−5.2
$F(g) + SiF_2{-}SiF_2{-}SiF_3(a) \rightarrow Si_2F_6(g)$	−6.9
$F(g) + SiF_2{-}SiF_2{-}SiF_3(a) \rightarrow Si_3F_8(g)$	−5.8

[a] The WWC reparmeterization of the SW potential is used to calculate ΔE for each chemical reaction. Details of the calculations of ΔE are given in the text.

III. Results of the Simulations

A. Mechanisms for Etching. The mechanisms for etching are determined by visually examining animations of the chemical reactions produced using a *Mathematica* notebook specifically designed for this purpose.[28] The primary mechanism observed for the formation of each of the etched products is an S_N2-like mechanism. At 7.0 and 9.0 eV, a secondary mechanism for the production of SiF_4 is observed in which the incoming fluorine atom inserts between the silicon−silicon bond.

1. F(g) + SiF₃(a). In agreement with previous simulations,[9] the primary mechanism for the production of SiF_4 is an S_N2-like mechanism. In this mechanism, the incoming fluorine atom approaches the middle of the adsorbate at an angle of 180° with respect to the silicon−substrate bond that is broken. As a bond forms between the incoming fluorine atom and the silicon atom, the adsorbate inverts with respect to the plane containing the three fluorine atoms. At 5.0 eV, fluorine atoms which approach the center of the silicon atom of the SiF_3 adsorbate are the most reactive and produce SiF_4 by an S_N2-like mechanism, while fluorine atoms that approach the surface around and/or near the adsorbate fluorine atoms are nonreactive. At 7.0 and 9.0 eV, the incoming fluorine atom has a greater amount of kinetic energy to overcome repulsion from the adsorbate fluorine atoms, and consequently, a wider area of aiming points produces SiF_4 by the S_N2-like mechanism. When the fluorine atom approaches the surface around the adsorbate, the adsorbate rotates toward the fluorine atom until the silicon atom is in a position to react by the S_N2-like mechanism. The incoming fluorine atom pulls the SiF_3 adsorbate toward it and removes it from the surface. Furthermore, at 7.0 and 9.0 eV, simulations show that some of the S_N2-like mechanisms actually involve the temporary displacement of an adsorbate fluorine atom. The adsorbate−fluorine atom bond breaks, and the fluorine forms a bond with the substrate silicon atom underneath the adsorbate. Once inversion of the adsorbate has taken place, this temporarily displaced fluorine atom reattaches itself to the adsorbate silicon atom and forms SiF_4, which then desorbs. The adsorbate fluorine atom facilitates reaction by replacing the dangling bond of the surface silicon atom as the silicon−substrate bond is broken.

At 7.0 and 9.0 eV, a higher energy mechanism for the formation of SiF_4 is observed in which the fluorine atom inserts underneath the adsorbate between the silicon−substrate bond. This mechanism takes place over a longer period of time than does the S_N2-like mechanism. In Figure 3, the fluorine atom bonds to the side of the adsorbate silicon atom to form a pentacoordinated SiF_4 intermediate complex at 56 fs. The complex sits on the surface for ∼150 fs. The adsorbate slowly rotates on the surface until the incoming fluorine atom can replace the silicon−substrate bond and bond to the silicon atom in a tetrahedral position. Finally, the incoming fluorine atom scoops underneath the adsorbate and pushes SiF_4 off of the surface.

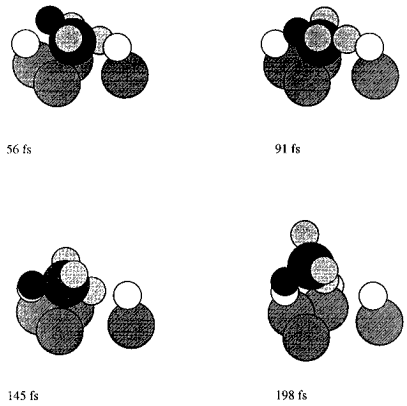

Figure 3. F and SiF_3 form SiF_4 through an intermediate complex at 7.0 eV. Silicon atoms are the spheres with the larger radii, and fluorine atoms are the spheres with the smaller radii. The pentacoordinated complex slowly rotates so that the incoming fluorine atom can replace the silicon−substrate bond and bond to SiF_3 in a tetrahedral position.

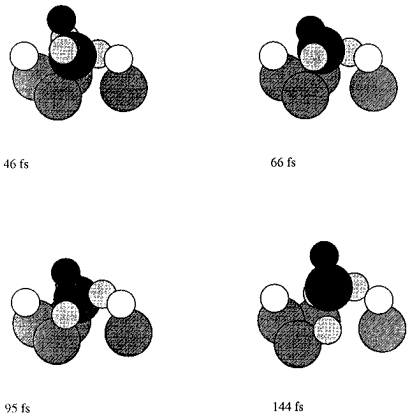

Figure 4. Displacement-type mechanism for the formation of SiF_3 at 7.0 eV in which the incoming fluorine atom displaces an adsorbate fluorine atom. The SiF_3 desorbs, leaving one of its fluorine atoms to replace the silicon−substrate bond.

At 7.0 and 9.0 eV, the radical SiF_3 is observed. Figure 4 shows the production of SiF_3 radical by a displacement-type mechanism whereby the incoming fluorine atom replaces an adsorbate fluorine atom. The incoming fluorine atom approaches the side of the adsorbate silicon atom and pushes down one of the adsorbate fluorine atoms, breaking the silicon−fluorine bond. The displaced fluorine atom rolls down to the substrate silicon atom that was bonded to the adsorbate, and SiF_3 desorbs from the surface.

2. F(g) + SiF₂ − SiF₃(a). As in the case of SiF_3, the primary mechanism for the formation of SiF_4 is an S_N2-like mechanism, which is the only mechanism observed at 5.0 eV. At 7.0 and 9.0 eV, some of the S_N2-like reactions involve the temporary displacement of an adsorbate fluorine atom, which was also observed with the SiF_3 adsorbate. The adsorbate silicon−fluorine bond breaks, and the fluorine atom forms a temporary bond with the substrate silicon atom underneath the adsorbate. After the SiF_3 inverts, the displaced fluorine atom reattaches to the adsorbate and SiF_4 desorbs. At 7.0 and 9.0 eV, a secondary mechanism is observed for the formation of SiF_4 in which the incoming fluorine atom approaches the center of the $SiF_2{-}SiF_3$ adsorbate and inserts between the silicon−silicon bond of the adsorbate. In Figure 5, the incoming fluorine atom approaches the adsorbate and bonds to the upper SiF_3 group, forming a pentacoordinated complex. Then, the upper SiF_3 group rotates so that the incoming fluorine atom can insert between the silicon−silicon bond and form tetrahedral SiF_4, which desorbs off of the surface.

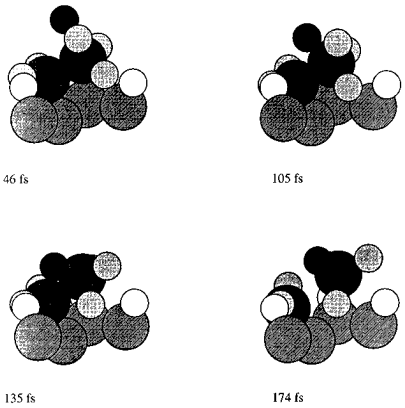

Figure 5. Insertion-type mechanism for the formation of SiF_4 from SiF_2-SiF_3 at 7.0 eV. The fluorine atom bonds to the top silicon atom at 105 fs. The top SiF_3 group rotates so that the fluorine atom can insert between the silicon−silicon bond and bond in a tetrahedral position to form SiF_4, which desorbs off of the surface.

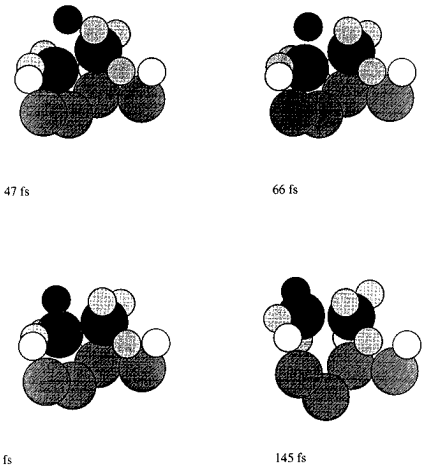

Figure 6. S_N2-like mechanism for the formation of Si_2F_6 from SiF_2-SiF_3 at 7.0 eV. As the incoming fluorine atom bonds to the bottom silicon atom of the adsorbate, the two fluorine atoms and the SiF_3 group undergo inversion.

The other major product, Si_2F_6, is also formed by an S_N2-like mechanism in which the fluorine atom approaches the silicon atom at an angle of 180° with respect to the silicon−substrate bond. However, this mechanism is different than that for the formation of SiF_4, because steric hindrance prevents a complete umbrella-like inversion from taking place. Figure 6 shows the incoming fluorine atom, which hits the bottom silicon atom and then bonds to it, thus replacing the adsorbate−substrate silicon bond. As this bond forms, the two fluorine atoms and the SiF_2 group undergo a slight inversion, which causes the silicon−silicon bond to stretch. The high exothermicity of the reaction can go either into the substrate or into the gas-phase product. Most of the excess energy is disposed into the product molecule, which strongly vibrates as it desorbs from the surface. In addition, at 9.0 eV, some of the Si_2F_6 dissociates into two SiF_3 fragments as the product desorbs off of the surface. A minor product, Si_2F_5, is formed by a displacement mechanism like that observed with SiF_3 in which the incoming fluorine atom breaks a silicon−fluorine bond.

3. F(g) + SiF₂−SiF₂−SiF₃(a). With $SiF_2-SiF_2-SiF_3$(a), an S_N2-like mechanism is responsible for all three major products: SiF_4, Si_2F_6, and Si_3F_8. Usually, a fluorine atom which hits the top silicon atom produces SiF_4, a fluorine atom which hits the middle silicon atom produces Si_2F_6, and a fluorine atom which hits the bottom silicon atom produces Si_3F_8. At 7.0 and 9.0 eV, SiF_4 is also produced by an insertion-type mechanism.

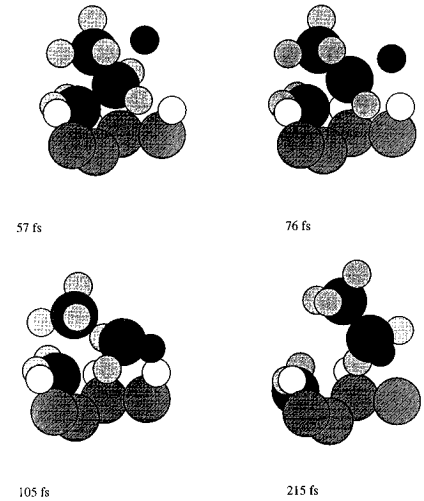

Figure 7. S_N2-type mechanism for the formation of Si_2F_6 from $SiF_2-SiF_2-SiF_3$ at 9.0 eV. The incoming fluorine atom pulls the middle silicon atom toward it so that it is in a good configuration to bond. As a result, two silicon−silicon bonds are broken at 105 fs. The silicon−silicon bond in Si_2F_6-reforms as it desorbs from the surface.

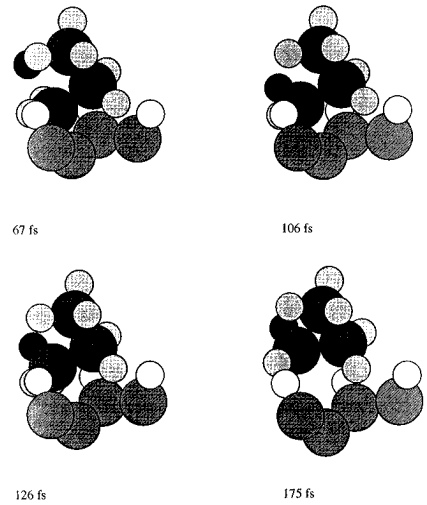

Figure 8. S_N2-type mechanism for the formation of Si_3F_8 from $SiF_2-SiF_2-SiF_3$ at 7.0 eV. The incoming fluorine atom bonds to the bottom silicon atom and abstracts the adsorbate.

The S_N2-like mechanism for the production of Si_2F_6 is shown in Figure 7. As the incoming fluorine atom approaches the side of the adsorbate, it attacks the back side of the middle adsorbate silicon atom. In order to have a favorable position for S_N2-attack, the incoming fluorine atom pulls the SiF_2 part of adsorbate toward it so that it rotates and breaks the SiF_2-SiF_3 bond. As the bond forms between the silicon atom and the incoming fluorine atom, the SiF_2 adsorbate becomes a leaving group, and the Si_2F_6 desorbs from the surface. One trajectory at 9.0 eV produces Si_2F_6 by hitting the top silicon atom in the adsorbate. Figure 8 illustrates the production of Si_3F_8. The fluorine atom approaches the bottom adsorbate silicon atom. As the silicon−fluorine bond forms, the adsorbate−substrate bond is broken and Si_3F_8 desorbs off of the surface. As in the case of the other radicals, both SiF_3 and Si_3F_7 are produced by a displacement-type mechanism.

B. Reaction Cross Section. *1. F(g) + SiF₃(a).* The total reaction cross section, SiF_3 cross section, and SiF_4 cross sections are shown in Table 2 at kinetic energies of 5.0, 7.0, and 9.0 eV. SiF_4 is the major product at all kinetic energies of the incoming fluorine atom. The energy threshold for the production of SiF_4 by the S_N2-like mechanism is ∼5.0 eV. This barrier

TABLE 2: Reaction Cross Section as a Function of Incident Kinetic Energy[a]

A. $F(g) + SiF_3(a)$

incident kinetic energy (eV)	reaction cross section (Å^2)			
	total	SiF_4 by S_N2	SiF_4 by insertion	SiF_3
3.0	no reaction			
5.0	0.6	0.6	0.0	0.0
7.0	3.7	3.3	0.1	0.3
9.0	4.4	3.3	0.6	0.5

B. $F(g) + SiF_2{-}SiF_3(a)$

incident kinetic energy (eV)	reaction cross section (Å^2)					
	total	SiF_4 by S_N2	SiF_4 by insertion	Si_2F_6	Si_2F_5	dissociated Si_2F_6
3.0	1.2	0.0	0.0	1.2	0.0	0.0
5.0	2.8	0.1	0.0	2.7	0.0	0.0
7.0	8.0	2.0	0.6	5.2	0.1	0.0
9.0	10.0	3.0	1.3	4.5	1.0	0.2

C. $F(g) + SiF_2{-}SiF_2{-}SiF_3(a)$

incident kinetic energy (eV)	reaction cross section (Å^2)							
	total	SiF_4 by S_N2	SiF_4 by insertion	Si_2F_6	Si_3F_8	Si_3F_7	SiF_3	dissociated Si_2F_6
3.0	no reaction							
5.0	2.9	1.8	0.0	0.7	0.4	0.0	0.0	0.0
7.0	5.6	3.1	0.5	0.8	1.2	0.0	0.0	0.0
9.0	8.7	3.5	0.8	2.7	0.7	0.2	0.2	0.4

[a] The reaction cross section and the reaction cross section for each of the major products are shown as a function of the incident kinetic energy with each adsorbate. The reaction cross section is calculated as the product of the fraction of trajectories that etch with the sampling area available to the incoming fluorine atom and has units of Å^2.

is caused by the inversion of SiF_3, which passes through an energetically unfavorable trigonal planar configuration. Consequently, no etching products are formed at 3.0 eV.

An S_N2-like mechanism is the only mechanism for the production of SiF_4 at 5.0 eV. The reaction cross section for the production of SiF_4 by the S_N2-like mechanism substantially increases by a factor of 5 from 5.0 to 7.0 eV. Above 7.0 eV, the additional trajectories which lead to reaction involve the insertion-type mechanism. The insertion-type mechanism accounts for 3% of the SiF_4 products at 7.0 eV and accounts for 15% of all SiF_4 products at 9.0 eV.

No SiF_3 radical is produced at 5.0 eV. At 7.0 eV, SiF_3 radical makes an 8% contribution, and at 9.0 eV, SiF_3 radical makes a contribution of 11%. SiF_3 is formed by a displacement mechanism in which a silicon−fluorine bond is broken. Consequently, as the kinetic energy of the incoming fluorine atom is increased to 7.0 eV, incoming fluorine atoms have a higher probability of displacing adsorbate fluorine atoms, and so the SiF_3 radical reaction cross section increases at the expense of the SiF_4 cross section.

2. F(g) + SiF$_2$−SiF$_3$(a). Table 2 shows the total reaction cross section and the reaction cross section of SiF_4, Si_2F_5, and Si_2F_6 and dissociated Si_2F_6 as a function of incident kinetic energy of the incoming fluorine atom. Si_2F_6 is the major product at all incident kinetic energies. The barrier to inversion for Si_2F_5 is lower than for SiF_3. Therefore, the energy threshold for reaction is 3.0 eV, and Si_2F_6 is formed at 3.0 eV. At 5.0 eV, SiF_4 by the S_N2-like mechanism has a small cross section, which shows a dramatic increase by a factor of 20 from 5.0 to 7.0 eV. SiF_4 by the insertion-type mechanism has a small cross section at 7.0 eV, which doubles at 9.0 eV. The insertion-type mechanism accounts for 23% of the SiF_4 at 7.0 eV and 30% of the SiF_4 at 9.0 eV. The percentage of SiF_4 increases dramatically from 4% to 43% as the incident kinetic energy increases from 5.0 to 9.0 eV.

As the incident kinetic energy increases, Si_2F_6 accounts for a smaller percentage of products as the other pathways become significant. Si_2F_6 is the sole product at 3.0 eV but accounts for only 45% of the products at 9.0 eV. At 9.0 eV, the Si_2F_5 radical becomes a minor product and a small number of Si_2F_6 products fragment into SiF_3 radicals as they desorb from the surface. Si_2F_5 is formed when a silicon−fluorine bond is broken. Therefore, the Si_2F_6 cross section decreases slightly at the expense of the Si_2F_5 and dissociated Si_2F_6 cross sections.

3. F(g) + SiF$_2$−SiF$_2$−SiF$_3$(a). Table 2 shows the total reaction cross section and the reaction cross section of SiF_4, Si_2F_6, Si_3F_8, Si_3F_7, SiF_3, and dissociated Si_2F_6 as a function of incident kinetic energy. As in the case of SiF_3, no reactions are observed at 3.0 eV. SiF_4 is the major product at all incident kinetic energies.

At 5.0 eV, SiF_4 by the S_N2-like mechanism is the major product, accounting for 62% of all of the products. Above 5.0 eV, SiF_4 is also formed by an insertion-type mechanism, which accounts for 14% of the SiF_4 at 7.0 eV and 19% of the SiF_4 at 9.0 eV.

Si_2F_6 and Si_3F_8 are minor products at all kinetic energies. At 9.0 eV, the reaction cross section for the production of Si_2F_6 increases substantially and the percentage of Si_2F_6 increases to 31%. The reason for this dramatic increase is that many of the reactions that produce Si_2F_6 break the adsorbate−substrate bond and temporarily break the upper silicon−silicon bond of the adsorbate, which requires about 8 eV. In addition, this mechanism produces a substantial amount of SiF_3 fragments at 9.0 eV. Si_3F_8 accounts for 14% of the products at 5.0 eV and 8% at 9.0 eV.

C. Energy Distribution. Table 3 lists the average energies of the products. All of the gas-phase products carry a large amount of kinetic energy as they leave the surface. As the mass of the gas-phase product increases, the kinetic energy of the product increases. Interestingly, the kinetic energy of the products does not increase proportionately with the incident kinetic energy of the incoming fluorine atom. This suggests that most of the kinetic energy of the incoming fluorine atom is absorbed by the surface and that the kinetic energy of the product arises from the high exothermicity of the chemical reaction. The kinetic energy is partitioned into both the center of mass kinetic energy and the kinetic energy of the internal motion of the atoms in the molecule. More than half of the

TABLE 3: Energy Distribution of the Products[a]

incident kinetic energy (eV)	product	$\langle E_{pot}\rangle$ (eV)	$\langle E_{kin}\rangle$ (eV)	$\langle E_{cm}\rangle$ (eV)	$\langle E_{int}\rangle$ (eV)
		A. F(g) + SiF_3(a)			
5.0	SiF_4 by S_N2	−22.8	4.4	1.7	2.7
7.0	SiF_3	−18.1	3.5	1.8	1.7
	SiF_4 by S_N2	−22.6	4.8	1.9	2.9
	SiF_4 by insertion	−23.2	4.6	2.1	2.5
9.0	SiF_3	−17.3	4.3	2.2	2.1
	SiF_4 by S_N2	−22.2	5.5	2.1	3.4
	SiF_4 by insertion	−22.3	5.7	2.5	3.2
		B. F(g) + SiF_2−SiF_3(a)			
3.0	Si_2F_6	−39.9	4.2	1.3	2.9
5.0	SiF_4 by S_N2	−23.7	3.2	1.4	1.8
	Si_2F_6	−39.7	4.7	1.6	3.1
7.0	SiF_4 by S_N2	−23.0	4.3	1.4	3.0
	SiF_4 by insertion	−22.9	4.4	1.6	2.8
	Si_2F_5	−34.0	3.1	1.1	2.0
	Si_2F_6	−39.1	5.1	1.6	3.5
9.0	SiF_3 fragments	−18.0	2.2	1.0	1.2
	SiF_4 by S_N2	−22.4	5.1	1.6	3.5
	SiF_4 by insertion	−22.7	5.0	1.9	3.1
	Si_2F_5	−34.0	3.3	1.4	1.9
	Si_2F_6	−38.6	5.9	1.9	4.0
		C. F(g) + SiF_2−SiF_2−SiF_3(a)			
5.0	SiF_4	−23.0	3.7	0.9	2.8
	Si_2F_6	−39.8	4.4	1.6	2.8
	Si_3F_8	−55.5	5.4	1.8	3.6
7.0	SiF_4 by S_N2	−22.5	4.3	1.2	3.1
	SiF_4 by insertion	−22.7	4.5	1.7	2.8
	Si_2F_6	−39.2	4.6	1.4	3.2
	Si_3F_8	−55.1	6.0	1.9	4.1
9.0	SiF_3	−17.4	4.7	2.2	2.5
	SiF_3 fragments	−17.9	2.1	0.9	1.2
	SiF_4 by S_N2	−22.0	5.2	1.6	3.6
	SiF_4 by insertion	−22.6	5.2	1.7	3.5
	Si_2F_6	−38.5	5.5	1.7	3.8
	Si_3F_7	−50.2	3.4	1.3	2.1
	Si_3F_8	−54.9	6.3	1.9	4.4

[a] The potential energy (E_{pot}), kinetic energy (E_{kin}), center of mass kinetic energy (E_{cm}) and internal energy (E_{int}) are shown for the products of each reaction. The energies are averaged over all of the products.

kinetic energy of the products is incorporated into the internal energy, i.e., rotational and vibrational motion, of the molecule.

D. Effective Internal Energy. In Figure 9, the effective internal energy of each of the gas-phases products is plotted as a function of kinetic energy of the incoming fluorine atom. Figure 9a shows the effective internal energy of SiF_4 for the reaction with SiF_3. As the kinetic energy increases, the average effective internal energy increases, and more products will fragment. SiF_4 produced by the insertion-type mechanism has a slightly smaller average effective internal energy because the mechanism requires more energy. At 5.0 eV, none of the SiF_4 gas-phase products by the S_N2-like mechanism fragment; at 7.0 eV, 9% fragment, and at 9.0 eV, 67% fragment. At 5.0 and 7.0 eV, none of the SiF_4 produced by the insertion-type mechanism fragments; at 9.0 eV, 52% fragment.

The effective internal energy of SiF_4 and Si_2F_6 from the reaction with SiF_2−SiF_3 is plotted in Figure 9b. As in the case with SiF_3, the average effective energy increases with kinetic energy, and the SiF_4 produced by the insertion-type mechanism has lower effective internal energy than that produced by the S_N2-like mechanism. At 5.0 eV, none of the SiF_4 gas-phase products by the S_N2-like mechanism fragment; at 7.0 eV, 11% fragment, and at 9.0 eV, 89% fragment. At 5.0 and 7.0 eV, all of the SiF_4 products produced by the insertion-type mechanism are stable; at 9.0 eV, 78% fragment. Si_2F_6 is a much less stable product, and nearly 100% will fragment at all incident kinetic energies. This is primarily due to the fact that the silicon−fluorine bond that is formed to make Si_2F_6 is stronger than the silicon−silicon bond that breaks for dissociation. Therefore, as the silicon−fluorine bond is formed, the energy released into the molecule is enough for the molecule to dissociate into fragments. With SiF_4, on the other hand, the bond formed and the bond to be broken for fragmentation have the same bond strength. Secondly, the energy threshold for reaction is lower for Si_2F_6, and the reaction is more exothermic. Lastly, Si_2F_6 has more degrees of freedom and, therefore, can absorb a greater amount of internal energy as it leaves the surface than can SiF_4.

Figure 9c shows the effective internal energy of the gas-phase products SiF_4, Si_2F_6, and Si_3F_8 from the reaction with SiF_2−SiF_2−SiF_3. The average effective internal energy of SiF_4 by the S_N2-like mechanism increases with kinetic energy: 0% fragment at 5.0 eV, 42% fragment at 7.0 eV, and 60% fragment at 9.0 eV. The SiF_4 produced by the insertion-type mechanism is more stable, with 0% fragmentation at 5.0 eV, 17% fragmentation at 7.0 eV, and 40% fragmentation at 9.0 eV. Nearly 100% of both the Si_2F_6 and Si_3F_8 products fragment at all kinetic energies and are the major contributors to the observed radical species. Si_3F_8 has a higher average effective internal energy than Si_2F_6 because the silicon−silicon bond is 0.4 eV weaker. Furthermore, Si_3F_8 has a greater number of degrees of freedom, and, therefore, is able to accommodate more energy as it leaves the surface than is Si_2F_6.

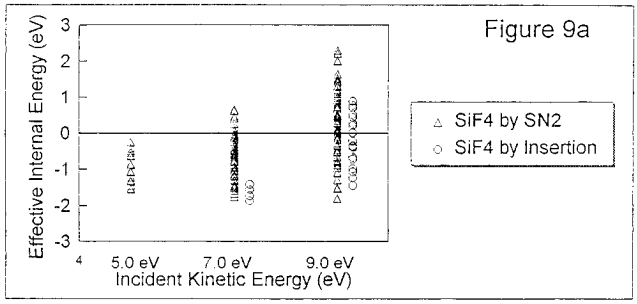

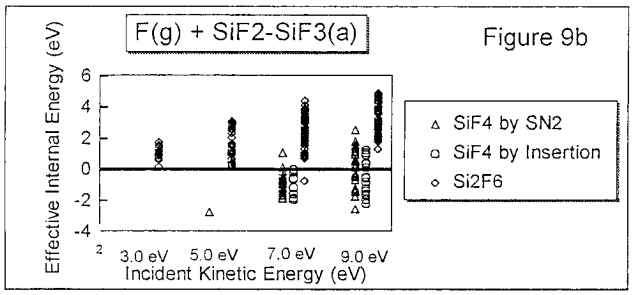

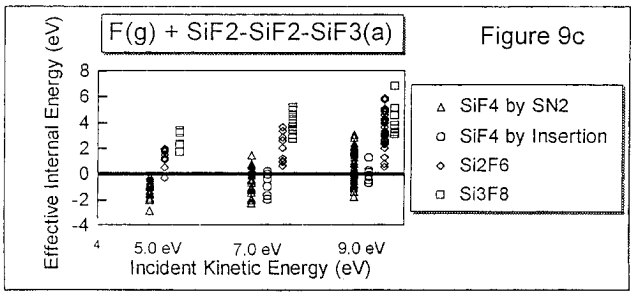

Figure 9. Effective internal energy (E_{eff}) of the gas-phase products. When E_{eff} is greater than zero, the product has enough energy to dissociate and will fragment into radicals before reaching the detector. (a) F(g) + SiF_3(a); (b) F(g) + SiF_2-SiF_3(a); (c) F(g) + $SiF_2-SiF_2-SiF_3$(a).

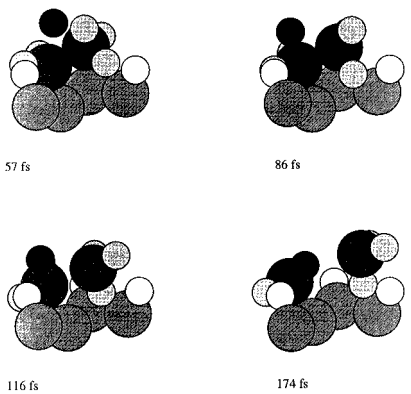

Figure 10. Chemically-induced desorption type mechanism for the formation of SiF_3 from SiF_2-SiF_3 at 9.0 eV. The incoming fluorine atom bonds to the lower silicon atom of the adsorbate, and the silicon−silicon adsorbate bond breaks. The upper SiF_3 rolls away from the adsorbate and desorbs, leaving SiF_3 on the surface.

E. Chemically-Induced Desorption. At 9.0 eV, a fair amount of chemically-induced desorption is observed with SiF_2-SiF_3 and $SiF_2-SiF_2-SiF_3$ in which the incoming fluorine atom displaces a portion or all of the adsorbate. The incoming fluorine atom adsorbs onto the surface, and the radical desorbs into the gas phase. With SiF_2-SiF_3, 6 of the 500 trajectories result in chemically-induced desorption of SiF_3 radicals, which have an average center of mass kinetic energy of 2.0 eV. Figure 10 illustrates the chemically-induced desorption mechanism for the production of SiF_3 with SiF_2-SiF_3. The incoming fluorine atom approaches the bottom silicon atom and bonds to it, thus breaking the adsorbate silicon−silicon bond. The upper SiF_3 fragments rolls away from the adsorbate and desorbs off of the surface, leaving the newly formed SiF_3 behind. With $SiF_2-SiF_2-SiF_3$ at 9.0 eV, chemically-induced desorption produces four SiF_3 radicals, three Si_2F_5 radicals, and two Si_3F_7 radicals. The center of mass kinetic energies for these products range from 1 to 3 eV.

IV. Discussion

Experiments on spontaneous silicon−fluorine etching at room temperature have shown that SiF_4 is the primary product and Si_2F_6 and Si_3F_8 are minor products, with the relative amounts of each product sensitive to surface conditions.[1−6] In our simulations, Si_2F_6 from SiF_2-SiF_3 is the only product at 3.0 eV. At 5.0 eV and above, SiF_4 is the primary product of the reaction with SiF_3 and with $SiF_2-SiF_2-SiF_3$. SiF_4 is a minor product with SiF_2-SiF_3 at 5.0 eV but becomes a substantial product at 7.0 and 9.0 eV. The simulations show that the product distribution will depend strongly on the relative amounts of each type of adsorbate, which is determined by the experimental conditions.

Almost all of the higher mass species, Si_2F_6 and Si_3F_8, are hyperthermal and have enough energy to fragment into smaller species. Our simulations predict that all of these species will fragment into radicals before reaching the detector. This is because the silicon−fluorine bond that is formed releases more energy into the product than the relatively smaller energy needed to break the silicon−silicon bond. Previous theoretical molecular dynamics simulations of etching with ion bombardment determined that the $(SiF_x)_n$ species may be buried deep within pits formed in the surface.[17,19] It is possible that the higher energy Si_2F_6 and Si_3F_8 collide with the walls of the pit as they desorb from the surface, thus releasing the extra energy and becoming stabilized. Simulations are performed to collide gas-phase products with a wall and show that collisions of the energetic species with a wall remove energy from the gas-phase products and stabilize them. In addition, because molecules are polarizable, it is likely that molecules which desorb at an angle from a planar surface will lose energy to the surface as well.

At higher kinetic energies, radicals are produced by both direct-etching reactions and chemically-induced desorption. However, the simulations predict that the primary source of radicals is the dissociation of higher mass species. In her study of the etching of n-type and p-type silicon, Houle observed that p-type silicon produces a greater flux of Si_2F_6 and SiF_3 than does n-type silicon.[4] The simulations have determined that the primary source of SiF_3 is the fragmentation of Si_2F_6 and, therefore, explains why an increase in flux of both SiF_3 and Si_2F_6 was observed.

The simulations predict some of the same gas-phase products as those observed in the experiments of Giapis *et al.*[10,11] Although thermal products were observed in the experiments, all of the products in our simulations are hyperthermal. With the high exothermicities of these reactions, it does not seem likely that the experimentally observed thermal products are formed by direct reactions between incoming fluorine atoms and adsorbed $(SiF_x)_n$ species. Our simulations predict three sources of hyperthermal SiF_3: etching, chemically-induced desorption, and fragmentation of higher mass species. Hyperthermal SiF_4 and SiF_2 are produced in our simulations by etching with $(SiF_x)_n$ species. In addition, hyperthermal SiF_2 may be produced by fragmentation of higher mass species.

Another finding of the simulations is the determination of the mechanisms responsible for the gas-phase products. The

primary mechanism for the formation of SiF_4 is an S_N2-like mechanism in which the incoming fluorine atom abstracts the top SiF_3 group, a mechanism that was determined previously from both molecular dynamics simulations[9] and *ab initio* calculations.[18] The simulations show that an S_N2-like mechanism is responsible for the formation of Si_2F_6 and Si_3F_8 as well. However, the simulations have discovered an additional mechanism for the formation of SiF_4 at 7.0 and 9.0 eV. This mechanism involves an insertion of the incoming fluorine atom between a silicon−silicon bond.

The sensitivity of the results to the potential used is an important indication of the reliability of the simulations. The WWC reparameterization predicts the silicon−silicon bond in gas-phase Si_2F_6 to be 4.4 eV, while the SW potential predicts the experimental value, 2.0 eV. Preliminary simulations show that the SW potential has a much higher reaction cross section and the energy threshold is lower. Furthermore, a higher percentage of the Si_2F_6 and Si_3F_8 products fragment into radicals as the gas-phase products leave the surface. Qualitatively, the mechanisms are the same with the two potentials. A comparison between the simulations with the SW and WWC potentials will be presented in a future paper. It should be noted that others have proposed that defects created by local heating play an essential role in silicon−fluorine etching.[7,8,21−23] The simulations in these studies use a crystalline substrate. Future studies will involve performing the same molecular dynamics simulations on a defective substrate in order to see the role of defects in promoting etching.

V. Conclusions

Molecular dynamics simulations of the reactions between hyperthermal fluorine atoms and SiF_3, SiF_2-SiF_3, and $SiF_2-SiF_2-SiF_3$ adsorbates on the Si{100}-(2×1) surface have been performed. Hyperthermal Si_2F_6 is observed at 3.0 eV. At 5.0 eV and above, hyperthermal SiF_4 is the major product and hyperthermal Si_2F_6 and Si_3F_8 are minor products. Small amounts of the radical species are observed, and this number increases substantially at 9.0 eV. SiF_4 is the most stable product, and the simulations predict that none will fragment at 5.0 eV. Nearly 100% of all Si_2F_6 and Si_3F_8 products have enough internal energy to dissociate into smaller fragments and are the primary contributors to the observed radical species. The molecular dynamics simulations support the hypothesis that the fluorosilyl layer consists of tower-like $(SiF_x)_n$ species, because reactions with these adsorbates do produce the experimentally observed products.

The simulations have determined that the primary mechanism for the formation of SiF_4 is an S_N2-like mechanism, which has also been determined by previous simulations. In addition, the simulations have discovered an additional mechanism for the production of SiF_4 at higher energies. Si_2F_6 and Si_3F_8 are formed by an S_N2-like mechanism.

Acknowledgment. Financial support of this work by the Department of Chemistry, College of Charleston, Research Corporation under Grant No. C-3499 and the National Science Foundation under a Research Planning Grant No. CHE-9409858 are gratefully acknowledged. We also thank Barbara Garrison, Konstantinos Giapis, Deepak Srivastava, Jory Yarmoff, and Paul Weakliem for interesting and useful discussions of this work.

References and Notes

(1) Winters, H. F.; Coburn, J. W. *Surf. Sci. Rep*. **1992**, *14*, 161−269.
(2) Winters, H. F.; Plumb, I. C. *J. Vac. Sci. Technol. B* **1991**, *9*, 197−207.
(3) Winters, H. F.; Haarer, D. *Phys. Rev. B.* **1987** *36*, 6613−6623.
(4) Houle, F. A. *J. Appl. Phys*. **1986**, *60*, 3018−3027.
(5) Stinespring, C. D.; Freedman, A. *Appl. Phys. Lett*. **1986**, *48*, 718−720.
(6) McFeely, F. R.; Morar, J. F.; Himpsel, F J. *Surf. Sci.* **1986**, *165*, 277−287.
(7) Lo, C. W.; Shuh, D. K.; Chakarian, V.; Durbin, T. D.; Varekamp, P. R.; Yarmoff, J. A. *Phys. Rev. B* **1993**, *47*, 15648−15659.
(8) Lo, C. W.; Varekamp, P. R.; Shuh, D. K.; Durbin, T. D.; Chakarian, V.; Yarmoff, J. A. *Surf. Sci*. **1993**, *292*, 171−181.
(9) Schoolcraft, T. A.; Garrison, B J. *J. Am. Chem. Soc.* **1991**, *113*, 8221−8228.
(10) Giapis, K. P.; Moore, T. A.; Minton, T. K. *J. Vac. Sci. Technol. A* **1995**, *13*, 959−965.
(11) K. P. Giapis, personal communication, 1995.
(12) Stillinger, F. H.; Weber, T. A. *Phys. Rev. B*, **1985**, *31*, 5262−5271.
(13) Stillinger, F. H.; Weber, T. A. *J. Chem. Phys*. **1988**, *88*, 5123−5133.
(14) Stillinger, F. H.; Weber, T. A. *Phys. Rev. Lett.* **1989**, *62*, 2144−2147.
(15) Weber, T. A.; Stillinger, F. H. *J. Chem. Phys*. **1990**, *92*, 6239−6245.
(16) Schoolcraft, T. A.; Garrison, B. J. *J. Vac. Sci. Technol. A* **1990**, *8*, 3496−3501.
(17) Feil, H.; van Zwol, J.; de Zwart, S. T.; Dieleman, J.; Garrison, B. J. *Phys. Rev. B* **1991**, *43*, 13695−13698.
(18) Garrison, B. J.; Goddard, W. A., III. *Phys. Rev. B* **1987**, *36*, 9805−9808.
(19) Barone, M. E.; Graves, D. B. *J. Appl. Phys*. **1995**, *77*, 1263−1274.
(20) Weakliem, P. C.; Wu, C. J.; Carter, E. A. *Phys. Rev. Lett*. **1992**, *69*, 200−203.
(21) Weakliem, P. C.; Carter, E. A. *J. Chem. Phys*. **1993**, *98*, 737−745.
(22) Carter, L. E.; Khodabandeh, S.; Weakliem, P. C.; Carter, E. A. *J. Chem. Phys*. **1994**, *100*, 2277−2288.
(23) Carter, L. E.; Carter, E. A. *J. Vac. Sci. Technol. A* **1994**, *12*, 2235−2239.
(24) Schoolcraft, T. A.; Diehl, A. M.; Steel, A. B.; Garrison, B. J. *J. Vac. Sci. Technol. A* **1995**, *13*, 1861−1866.
(25) Sommerer, T. J.; Kushner, M. J. *J. Appl. Phys.* **1991**, *70*, 1240−1251.
(26) Berendsen, H. J. C.; Postma, J. P.; van Gunsteren, W. F.; Dinola, A.; Haak, J.R. *J. Chem. Phys*. **1984**, *81*, 3684−3690.
(27) Taylor, R. S.; Garrison, B. J. *Langmuir* **1995**, *11*, 1220−1228.
(28) Acree, B.; McCormac, R.; Fullbright, G.; Weaver, S.; Krantzman, K. D. *J. Chem. Educ.* **1995**, *72*, 1077−1079.

JP960058T